Acta Crystallographica Section F
Structural Biology and Crystallization Communications
ISSN 1744-3091

Crystallization and preliminary X-ray crystallographic analysis of the tetracycline-degrading monooxygenase TetX2 from *Bacteroides thetaiotaomicron*

Gesa Volkers,[a]* Linda Schuldt,[a]‡ Gottfried J. Palm,[a] Gerard D. Wright[b] and Winfried Hinrichs[a]

[a]Institut für Biochemie, Universität Greifswald, Felix-Hausdorff-Strasse 4, D-17489 Greifswald, Germany, and [b]Michael G. DeGroote Institute for Infectious Disease Research, Department of Biochemistry and Biomedical Sciences, McMaster University, 1200 Main Street West, Hamilton, Canada

‡ Current address: EMBL, c/o DESY, Notkestrasse 85, D-22603 Hamburg, Germany.

Correspondence e-mail: gesa.volkers@uni-greifswald.de

Received 12 March 2010
Accepted 31 March 2010

The flavin-dependent monooxygenase TetX2 from *Bacteroides thetaiotaomicron* confers resistance against tetracyclines in aerobically grown *Escherichia coli*. TetX2 modifies several tetracycline antibiotics by regioselective hydroxylation of the substrates to 11a-hydroxy-tetracyclines. X-ray diffraction data were collected from a native TetX2 crystal and a TetX2 crystal with incorporated selenomethionine to resolutions of 2.5 and 3.0 Å, respectively. The native crystal belonged to the triclinic space group $P1$, with unit-cell parameters a = 68.55, b = 80.88, c = 87.53 Å, α = 111.09, β = 98.98, γ = 93.38°, whereas the selenomethionine-labelled TetX2 crystal belonged to the monoclinic space group $P2_1$, with unit-cell parameters a = 87.34, b = 68.66, c = 152.48 Å, β = 101.08°.

1. Introduction

Since their discovery in 1948 (Duggar, 1948), tetracycline antibiotics have been widely used against infections by Gram-positive and Gram-negative bacterial pathogens and cell parasites. The FAD-dependent monooxygenase TetX modifies several tetracycline antibiotics by regioselective hydroxylation of the substrates to 11a-hydroxy-tetracyclines, which further degrade non-enzymatically to as yet uncharacterized products (Yang *et al.*, 2004). The active enzyme requires molecular oxygen, NADPH and Mg^{2+} and has a broad tetracycline substrate range that includes the recently approved third-generation antibiotic tigecycline (Moore *et al.*, 2005). The resistance determinant *tetX* belongs to the tetracycline resistome. Only two other genes, *tet37* and *tet34*, have been associated with enzymatic tetracycline inactivation (Thaker *et al.*, 2010). When transferred to *Escherichia coli*, the expression of TetX results in a colour change of the cultivating medium to brown in the presence of tetracycline and molecular oxygen. The dark brown colour is believed to arise from a polymer formed by the unstable degradation product 11a-hydroxy-tetracycline at physiological pH. Hydroxylated tetracyclines show weaker antibiotic properties. This is an effect of their degradation (Moore *et al.*, 2005) and of the weaker coordination of magnesium ions, which is crucial for binding to the ribosome (Pioletti *et al.*, 2001).

Tetracycline inactivation by degradative hydroxylation is a new resistance mechanism which, in contrast to efflux or ribosomal protection mechanisms, is only partly understood. Until now, *tetX* has not been identified in clinically important pathogenic bacteria. The gene was found accidentally on transposons Tn*4351* and Tn*4400* in *Bacteroides fragilis* during the cloning and expression of an erythromycin-resistance gene, but does not confer resistance to its anaerobic host because of its dependency on molecular oxygen (Speer & Salyers, 1988). Orthologous genes *tet*X1 and *tet*X2 have been found on transposons CTnDOT in *B. thetaiotaomicron*. TetX1 and TetX2 share 61.7% and 99.5% sequence identity, respectively, with TetX from *B. fragilis*. *Tet*X has also been found in aerobic *Sphingobacterium* sp., with 99.8% nucleotide and 100% amino-acid identity to *tet*X2 of CTnDOT from *B. thetaiotaomicron*. It is assumed that *Sphingobacterium* is the ancestral source of the *tet*X genes (Ghosh *et al.*, 2009).

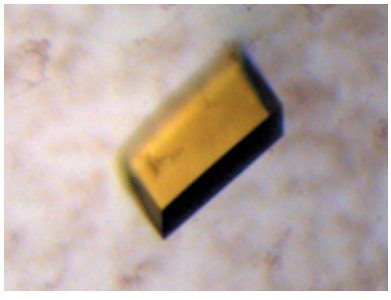

Table 1
Data-collection and processing statistics.

Values in parentheses are for the highest resolution shell.

		SeMet-labelled TetX2		
	Native TetX2	Peak	Inflection point	High-energy remote
Space group	*P*1	$P2_1$		
Unit-cell parameters (Å, °)	a = 68.55, b = 80.88, c = 87.53, α = 111.09, β = 98.98, γ = 93.38	a = 87.34, b = 68.66, c = 152.48, β = 101.08		
Resolution (Å)	43–2.5 (2.64–2.5)	99.0–3.0 (3.16–3.0)		
Wavelength (Å)	1.5418	0.97784	0.97838	0.95369
Crystal-to-detector distance (mm)	50	300		
Rotation range per image (°)	0.5	1		
Total rotation range (°)	360	360		
Exposure time per image (s)	20, 100, 100	20		
No. of measured reflections	225128	246652	246995	245329
No. of unique reflections	60153	35742	35857	35851
Multiplicity	3.7 (3.8)	6.9 (6.5)	6.9 (6.5)	6.8 (6.5)
Completeness (%)	99.6 (100)	99.5 (98.8)	99.4 (98.5)	99.2 (97.8)
Mean $I/\sigma(I)$	5.1 (2.5)	11.7 (2.9)	11 (2.5)	9.8 (2.0)
$R_{\rm r.i.m.}$† (%)	19.1 (57.4)	21.9 (72.9)	21.7 (76.8)	29.9 (89.3)
$R_{\rm p.i.m.}$‡ (%)	9.8 (29.4)	8.0 (26.8)	8.0 (28.4)	10.8 (32.1)
Mosaicity (°)	2.5§	0.7	0.71	0.71
Overall B factor from Wilson plot (Å^2)	53.9	53.8	55.4	58.6

† $R_{\rm r.i.m.} = \sum_{hkl}[N/(N-1)]^{1/2}\sum_i |I_i(hkl) - \langle I(hkl)\rangle|/\sum_{hkl}\sum_i I_i(hkl)$. ‡ $R_{\rm p.i.m.} = \sum_{hkl}[1/(N-1)]^{1/2}\sum_i |I_i(hkl) - \langle I(hkl)\rangle|/\sum_{hkl}\sum_i I_i(hkl)$. § The mosaicity was fixed at 1.0° for integration and processing.

The multiple-wavelength anomalous dispersion technique (Hendrickson, 1991) with selenomethionine-labelled crystals was chosen for structure solution, as recombinant TetX2 protein contains 11 methionine residues which lead to a sufficient anomalous signal. Phasing by molecular replacement with the closest structurally known relative, PhzS hydroxylase from *Pseudomonas aeruginosa* (PDB entry 3c96; S. M. Vorobiev, Y. Chen, J. Seetharaman, D. Wang, L. Mao, R. Xiao, T. B. Acton, G. T. Montelione, L. Tong & J. F. Hunt, unpublished work), was not successful; the sequence identity of PhzS hydroxylase to TetX2 monooxygenase is 24.8%. Here, we report the crystallization and preliminary X-ray diffraction analysis of TetX2 from *B. thetaiotaomicron*.

2. Experimental methods

2.1. Protein expression and purification

The *tet*X2 gene was inserted into the T7 promoter-driven expression vector pET-28b(+) (Novagen), resulting in an N-terminal His_6 tag. The recombinant protein consists of 398 amino acids with a molecular weight of 44 660 Da, starting with Met11 from the original protein sequence and an N-terminal extension (MGSSHHHHHS-SGLVPRGSH). The vector construct was introduced into *E. coli* strain BL21 (DE3) for native expression and B834 pRare2 competent cells for selenomethionine (SeMet) labelling, respectively. Transformants were selected on LB agar plates containing 50 µg ml^{-1} kanamycin and were cultured at 310 K in liquid LB medium with the same concentration of kanamycin. Cells from a 5 ml overnight culture of BL21 (DE3) pET-28(*tet*X2) were used to inoculate 500 ml LB [or a 5 ml B843 pRARE2 pET-28(*tet*X2) culture was used to inoculate 500 ml minimal medium M9 containing 50 mg l^{-1} L-selenomethionine in the case of the labelled protein] in the presence of kanamycin. To produce soluble protein, the cells were subsequently cooled to 287 K when a cell density (OD_{600}) of 0.5 was reached. Expression of the recombinant protein was induced with isopropyl β-D-1-thiogalactopyranoside at a final concentration of 1 m*M*. After an expression time of 20 h, cells were pelleted by centrifugation at 9720*g* for 10 min and stored at 253 K until further processing. 2 ml buffer containing 1 m*M* EDTA, 10 m*M* imidazole, 500 m*M* NaCl, 50 m*M* HEPES pH 7.5, 0.1 m*M* PMSF and 0.07% β-mercaptoethanol per gram of wet cell pellet was used for resuspension. Cell lysis was performed by three passes through a French press. The homogenate was centrifuged for

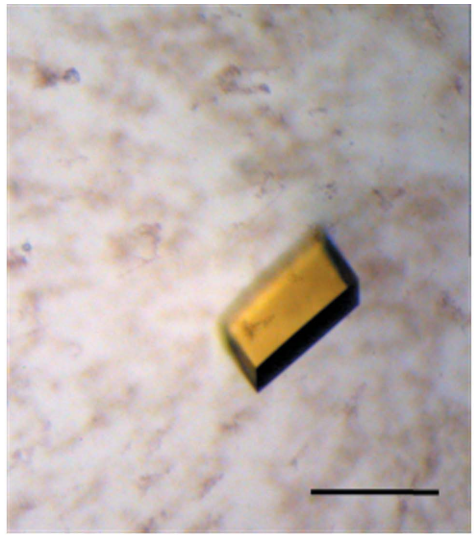

(*a*)

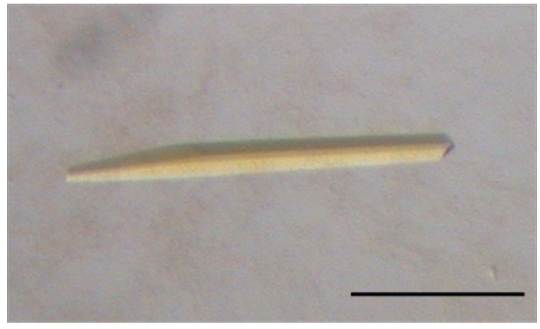

(*b*)

Figure 1
Crystals of TetX2 from *B. thetaiotaomicron*. (*a*) Native TetX2 crystal. (*b*) Crystal of SeMet-labelled TetX2 protein. The yellow colour results from the bound FAD cofactor. The solid bar represents 0.1 mm.

1 h at 48 000*g* and 277 K. The supernatant was filtered through a 0.2 µm syringe filter and loaded onto an Ni^{2+}-charged immobilized metal-affinity column (Poros 20 MC, Applied Bioscience) equilibrated with 50 m*M* HEPES pH 7.5, 500 m*M* NaCl, 10 m*M* imidazole. Elution was achieved by applying a linear gradient of 10–250 m*M* imidazole in the same buffer. Fractions containing TetX2 were pooled and dialyzed for 30 min against pure water and for 90 min against 20 m*M* HEPES pH 8.0, 10% glycerol. The protein was then loaded onto an anion-exchange chromatography column (Poros 20 HQ, Applied Bioscience) equilibrated with 20 m*M* HEPES pH 8.0 and eluted with 20 m*M* HEPES pH 8.0, 1000 m*M* NaCl. TetX2-containing fractions were concentrated to 1–2 ml by ultrafiltration using an Amicon Millipore filter unit (molecular-weight cutoff 10 000) and subsequently loaded onto a gel-filtration column (Superdex200, GE Healthcare) equilibrated with 20 m*M* HEPES pH 8.0, 100 m*M* NaCl. After dialysis against 20 m*M* HEPES pH 7.0, the TetX2 protein was concentrated to the desired concentration by ultrafiltration and crystallization experiments were carried out. Protein concentration was determined using a modified Bradford method (Roti-Nanoquant, Roth; Zor & Selinger, 1996).

2.2. Crystallization

The TetX2 protein was screened for initial crystallization conditions by the sitting-drop vapour-diffusion method using an HTPC crystallization robot (CyBio), 96-well plates (CrystalQuick Lp, Greiner Bio-One) and sparse-matrix screens based on commercially available screens (Hampton Research, Jena Bioscience). Initial hits were optimized in 24-well crystallization plates (Greiner Bio-One) with the hanging-drop vapour-diffusion method. Each well contained 500 µl reservoir solution. After optimization, crystals of native TetX2 protein [10 mg ml^{-1} TetX2 in 20 m*M* HEPES pH 7.0, 0.2 m*M* flavin adenine dinucleotide (FAD), 1 m*M* $MgCl_2$, 30 m*M* DTT] were obtained using a reservoir solution consisting of 1.8 *M* ammonium sulfate and 30 m*M* sodium citrate buffer. SeMet-labelled TetX2 (4 mg ml^{-1} TetX2 in 20 m*M* HEPES pH 7.0, 0.2 m*M* FAD, 1 m*M* $MgCl_2$ and 30 m*M* DTT) crystallized in the presence of 1.4 *M* ammonium sulfate and 100 m*M* sodium citrate buffer pH 7 at 293 K. For the hanging drops, 2 µl native protein solution was mixed with 1 µl reservoir solution. In the case of SeMet-labelled protein the drops were composed of 2 µl protein solution, 4 µl water and 1 µl reservoir solution. Crystallization trays and solutions were kept on ice during crystallization set-up.

2.3. Data collection and processing

Diffraction data from a single TetX2 crystal were collected to a resolution of 2.5 Å in-house at the Cu $K\alpha$ wavelength using a Rigaku/MSC X-ray source with a MicroMax-007 rotating-anode generator and multilayer optics (beam size 0.3 × 0.3 mm, Osmic) and a CCD detector (Saturn 92, Rigaku/MSC). The crystal was transferred into and soaked in a cryoprotectant-containing reservoir solution [15%(*v*/*v*) glycerol] and flash-cooled to 110 K (Oxford Cryosystems). Three scans were performed and the collected data were merged. For the native TetX2 data the program *CrystalClear* v.1.3.6 (Pflugrath, 1999) was used for indexing and integration and *SCALA* from the *CCP*4 suite (Collaborative Computational Project, Number 4, 1994) was used for scaling. The mosaicity was fixed at 1.0° during processing. The 3.6–3.8 Å resolution shell was removed during integration because of an ice ring. SeMet-labelled TetX2 was employed in a multiple-wavelength anomalous dispersion (MAD) experiment on EMBL beamline X12 at the DESY synchrotron source (Hamburg) equipped with a MAR CCD 225 detector.

The cryoprotectant for SeMet-labelled crystals consisted of reservoir solution with 20% glycerol and flash-cooling was performed in liquid nitrogen before mounting. Three data sets were collected from one SeMet-labelled TetX2 crystal using wavelengths around the selenium absorption edge as verified by a fluorescence scan, namely

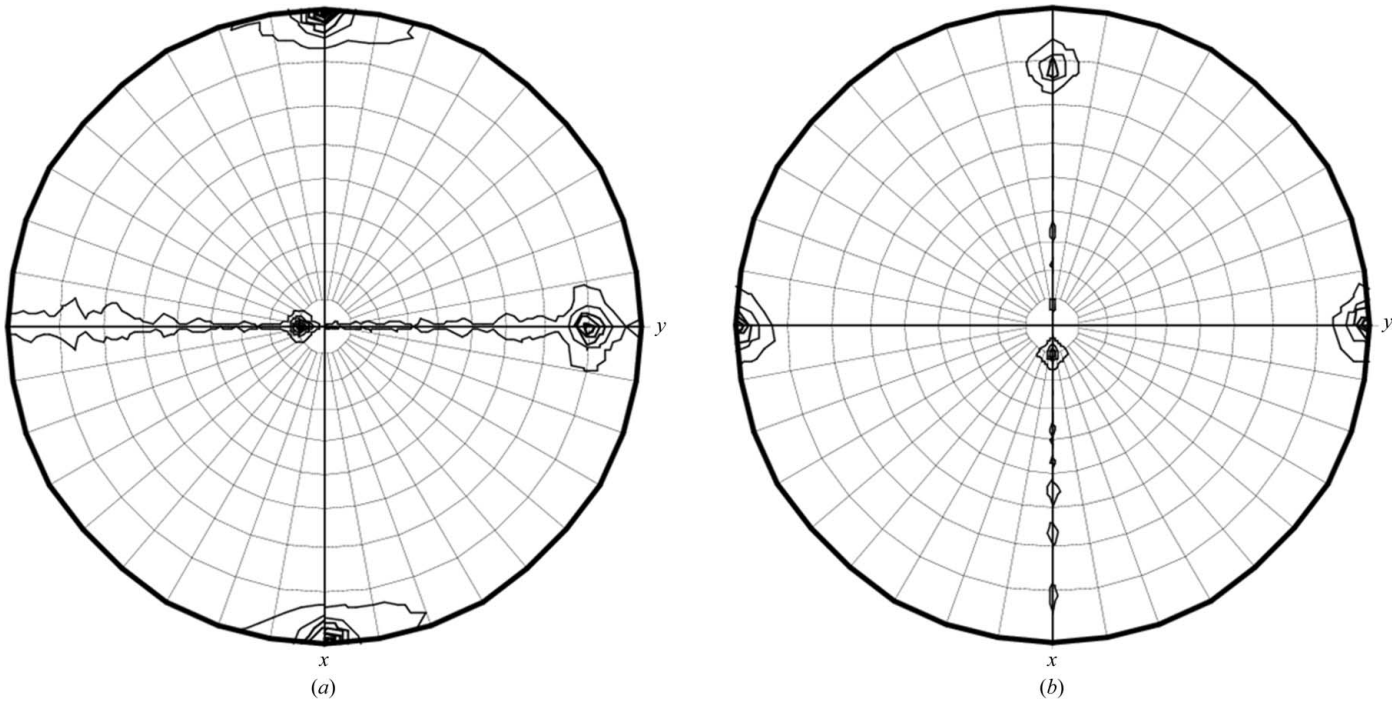

Figure 2
Self-rotation function in the $\kappa = 180^\circ$ section, revealing two independent twofold noncrystallographic axes in both unit cells. (*a*) Native TetX2 crystal in space group *P*1. (*b*) SeMet-labelled TetX2 crystal in space group $P2_1$. The plots were created with *MOLREP* (Collaborative Computational Project, Number 4, 1994).

at the peak (0.97784 Å), the inflection point (0.97838 Å) and a high-energy remote (0.95369 Å). *DENZO* and *SCALEPACK* from the *HKL*-2000 package (Otwinowski & Minor, 1997) were used for processing of the MAD data. To obtain values for $R_{\rm r.i.m.}$ (the redundancy-independent merging *R* factor) and $R_{\rm p.i.m.}$ (the precision-indicating merging *R* factor) (Weiss, 2001), the MAD data were processed with *MOSFLM* and *SCALA* from the *CCP*4 suite (Collaborative Computational Project, Number 4, 1994). Structure-factor amplitudes were obtained from intensities with *TRUNCATE* (French & Wilson, 1978; Collaborative Computational Project, Number 4, 1994). Table 1 displays the important parameters of data collection and processing.

2.4. Structure solution

Successful initial phasing was directly possible at the beamline using the *Auto-Rickshaw* protocol (Panjikar *et al.*, 2005), which incorporates *CAD* (Collaborative Computational Project, Number 4, 1994), *SCALEIT* (Collaborative Computational Project, Number 4, 1994), *SHELXC* (Sheldrick, 2008), *SHELXD* (Sheldrick, 2008), *SHARP* (Bricogne *et al.*, 2003), *DM* (Cowtan, 1994), *RESOLVE* (Terwilliger, 2000) and *HELICAP* (Morris *et al.*, 2004). The selenium positions identified during the *Auto-Rickshaw* process were used to determine noncrystallographic symmetry axes with *NCSFIND* (Collaborative Computational Project, Number 4, 1994) and further correction and completion of the selenium positions was carried out based on this information. After phase improvement and density modification with *SHARP*, initial model building was performed manually in *Coot* (Emsley & Cowtan, 2004). Based on structure-factor amplitudes, the self-rotation function in the $\kappa = 180^\circ$ section was calculated with *MOLREP* (Collaborative Computational Project, Number 4, 1994) to a maximum resolution of 6 Å.

3. Results and discussion

The yield of SeMet-labelled TetX2 protein was similar to the expression of wild-type TetX2 (∼5 mg protein per litre of culture). In both cases crystals appeared amid precipitate within a period of three weeks (Fig. 1). Lowering the protein concentration to prevent precipitation inhibited crystallization. Native TetX2 crystallized in the triclinic space group *P*1 and SeMet-labelled TetX2 crystallized in the monoclinic space group $P2_1$.

The asymmetric unit of the $P2_1$ unit cell consists of four monomers as indicated by the Matthews coefficient ($V_{\rm M}$) of 2.59 Å^3 Da^{-1}, corresponding to a calculated solvent content of 52.4% (Matthews, 1968). The unit cell of the native TetX2 crystal in *P*1 consists of four monomers which are arranged in a similar way as in the $P2_1$ unit cell (Matthews coefficient $V_{\rm M}$ = 2.60 Å^3 Da^{-1}, solvent content 52.5%). Of the 44 expected Se atoms in the asymmetric unit of the $P2_1$ unit cell, 43 were located by *SHELXD* [CC(all) = 37.63; CC(weak) = 18.93]. Two independent twofold noncrystallographic axes were confirmed. The self-rotation function also indicates two independent twofold noncrystallographic axes in the unit cells of both the native and the SeMet-labelled TetX2 crystals, but with a slightly different orientation of the four monomers in the *P*1 and the $P2_1$ unit cells (Fig. 2). Model refinement against the native data is currently in progress and structural details will be presented elsewhere. This is the first report of the crystallization and structure solution of a tetracycline-degrading monooxygenase.

References

Bricogne, G., Vonrhein, C., Flensburg, C., Schiltz, M. & Paciorek, W. (2003). *Acta Cryst.* D**59**, 2023–2030.
Collaborative Computational Project, Number 4 (1994). *Acta Cryst.* D**50**, 760–763.
Cowtan, K. (1994). *Jnt CCP4/ESF–EACBM Newsl. Protein Crystallogr.* **31**, 34–38.
Duggar, B. M. (1948). *Ann. N. Y. Acad. Sci.* **51**, 177–181.
Emsley, P. & Cowtan, K. (2004). *Acta Cryst.* D**60**, 2126–2132.
French, S. & Wilson, K. (1978). *Acta Cryst.* A**34**, 517–525.
Ghosh, S., Sadowsky, M. J., Roberts, M. C., Gralnick, J. A. & LaPara, T. M. (2009). *J. Appl. Microbiol.* **106**, 1336–1342.
Hendrickson, W. A. (1991). *Science*, **254**, 51–58.
Matthews, B. W. (1968). *J. Mol. Biol.* **33**, 491–497.
Moore, I. F., Hughes, D. W. & Wright, G. D. (2005). *Biochemistry*, **44**, 11829–11835.
Morris, R. J., Zwart, P. H., Cohen, S., Fernandez, F. J., Kakaris, M., Kirillova, O., Vonrhein, C., Perrakis, A. & Lamzin, V. S. (2004). *J. Synchrotron Rad.* **11**, 56–59.
Otwinowski, Z. & Minor, W. (1997). *Methods Enzymol.* **276**, 307–326.
Panjikar, S., Parthasarathy, V., Lamzin, V. S., Weiss, M. S. & Tucker, P. A. (2005). *Acta Cryst.* D**61**, 449–457.
Pioletti, M., Schlünzen, F., Harms, J., Zarivach, R., Glühmann, M., Avila, H., Bashan, A., Bartels, H., Auerbach, T., Jacobi, C., Hartsch, T., Yonath, A. & Franceschi, F. (2001). *EMBO J.* **20**, 1829–1839.
Pflugrath, J. W. (1999). *Acta Cryst.* D**55**, 1718–1725.
Sheldrick, G. M. (2008). *Acta Cryst.* A**64**, 112–122.
Speer, B. S. & Salyers, A. A. (1988). *J. Bacteriol.* **170**, 1423–1429.
Terwilliger, T. C. (2000). *Acta Cryst.* D**56**, 965–972.
Thaker, M., Spanogiannopoulos, P. & Wright, G. D. (2010). *Cell. Mol. Life Sci.* **67**, 419–431.
Weiss, M. S. (2001). *J. Appl. Cryst.* **34**, 130–135.
Yang, W., Moore, I. F., Koteva, K. P., Bareich, D. C., Hughes, D. W. & Wright, G. D. (2004). *J. Biol. Chem.* **279**, 52346–52352.
Zor, T. & Selinger, Z. (1996). *Anal. Biochem.* **236**, 302–308.